

# Spectroscopic Assessment of Doxorubicin (DOX)-Gemcitabine (GEM) Gold Complex Nanovector as Diagnostic Tool of Galectin-1 Biomarker

Memona Khan\*, Khaoula Cherni\*, Rawdha Dekhili, Jolanda Spadavecchia 

CNRS, UMR 7244, NBD-CSPBAT, Laboratory of Chemistry, Structures and Properties of Biomaterials and Therapeutic Agents University Paris 13, Sorbonne Paris Nord, Bobigny, France

\*These authors contributed equally to this work

Correspondence: Rawdha Dekhili; Jolanda Spadavecchia, Email rawdhadekhillichimiste@gmail.com; jolanda.spadavecchia@univ-paris13.fr; jolanda.spadavecchia@gmail.com

**Introduction:** The aim of this study is focused on the development of theranostic hybrid nanovectors based on gold-doxorubicin (DOX)-gemcitabine (GEM) complexes and their active targeting with Galectin-1 (Gal-1) as a promising therapeutic and prognostic marker in cancer.

**Methods:** For this purpose, a gold salt ( $\text{HAuCl}_4$ ) interacts with antitumor drugs (DOX; GEM) by chelation and then stabilizes with dicarboxylic acid-terminated polyethylene glycol (PEG) as a biocompatible surfactant. The proposed methodology is fast and reproducible, and leads to the formation of a hybrid nanovector named GEM@DOX IN PEG-AuNPs, in which the chemobiological stability was improved. All synthetic chemical products were evaluated using various spectroscopic techniques (Raman and UV-Vis spectroscopy) and transmission electron microscopy (TEM).

**Results:** To conceive a therapeutic application, our hybrid nanovector (GEM@DOX IN PEG-AuNPs) was conjugated with the Galectin-1 protein (Gal-1) at different concentrations to predict and specifically recognize cancer cells. Gal-1 interacts with GEM@DOX in PEG-AuNPs, as shown by SPR and Raman measurements. We observed both dynamic variation in the plasmon position (SPR) and Raman band with Gal-1 concentration.

**Discussion:** We identified that GEM grafted electrostatically onto DOX IN PEG-AuNPs assumes a better chemical conformation, in which the amino group ( $\text{NH}_3^+$ ) reacts with the carboxylic ( $\text{COO}^-$ ) group of PEG diacid, whereas the cyclopentanol group at position C-5' reacts with  $\text{NH}_3^+$  of DOX.

**Conclusion:** This study opens further way in order to built “smart nanomedical devices” that could have a dual application as therapeutic and diagnostic in the field of nanomedicine and preclinical studies associated.

**Keywords:** gold-complex, gemcitabine, doxorubicin, galectin-1 protein, Raman spectroscopy, nanovector, diagnostic, biomarkers

## Introduction

Gold nanoparticles (AuNPs) are extensively used in several fields such as nanomedical devices, nano-drug delivery systems,<sup>1</sup> and nanosensors.<sup>2</sup> The opto- and physico-chemical properties of AuNPs, such as localized surface plasmon resonance (LSPR), allow their implementation in therapy and diagnostics<sup>3</sup> because of their capacity to convert irradiated energy into thermal energy, resulting in the release of toxic radicals at high temperatures (photodynamic therapy).<sup>4</sup> Owing to their unique optical versatility and fast surface modification, many authors have studied original and specific chemical functionalization protocols<sup>5</sup> to realize accurate drug carriers for cancer theranostics.<sup>6</sup> In recent years, Spadavecchia et al developed a library of drug delivery systems (DDS) based on chemotherapeutic and/or biomolecule-gold-complexes using an experimental approach

named “Method IN”.<sup>7–11</sup> They also investigated the chelation process of doxorubicin (DOX) with gold salt<sup>7,9,10</sup> and the electrostatic approach of gemcitabine (GEM) onto pegylated gold nanoparticles, before reduction, in order to form metallo nanoflower. In this way, GEM was adsorbed onto different gold facets [1.1.0] during nucleation and growth process of AuNPs.

Some authors have conceived hybrid AuNPs based on chitosan and chitosan derivatives<sup>12</sup> as sugar stabilizers for the detection of galectin-1 protein as a cancer biomarker<sup>13</sup> in several fields of nanomedicine.<sup>14</sup> Galectin-1 (Gal-1) is expressed in several tissues and is involved in an extensive range of biological processes.<sup>15</sup>

Recently, various analytical methods have been suggested for the detection of galectin, based on electrochemical and localized surface plasmon resonance.<sup>16</sup> Most of these methods are expensive owing to the need for specific antibodies.<sup>17</sup>

Previously, we have investigated the interactions between CTL polymer-decorated AuNPs and Gal-1<sup>13</sup>. Herein, we demonstrate how the steric arrangement of chemotherapeutics such as DOX and GEM can influence the chemical interaction of Gal-1. The properties of DOX-GEM complex nanovectors and their ability to specifically target galectin-1 were studied. This interaction was confirmed using Surface Plasmon Resonance (LSPR), transmission electron microscopy (TEM)<sup>18</sup> and Raman spectroscopy as physicochemical characterizations.

The results of this study may provide valuable information regarding the use of these nanovectors as diagnostic tools for early detection of galectin-1 as a biomarker in cancer therapy.

## Experimental Section

### Materials and Methods

Tetrachloroauric acid ( $\text{HAuCl}_4 \cdot 3\text{H}_2\text{O}$ ), sodium borohydride ( $\text{NaBH}_4$ ), dicarboxylic Polyethylene Glycol (PEG)-600 (PEG) (PEG-diacide), phosphate buffered saline (PBS, 0.1 M, pH from 4 to 13), DMEM, Doxorubicin (DOX) (98%), and Gemcitabine (GEM) (98%), were purchased from Sigma Aldrich. Recombinant Human Galectin-1 (Lot# 0707271–1) was purchased from PeprTech (Rocky Hill, NJ).

### Synthesis of DOX in-PEG-AuNPs

DOX IN PEG-AuNPs colloids were synthesized using a slight modification of the protocol described previously.<sup>7</sup> Briefly, 20 mL of  $\text{HAuCl}_4$  solution (0.08M) was mixed with DOX (5 mL, 0.1M) and stirred for 20 min. Subsequently, 250  $\mu\text{L}$  of dicarboxylic PEG was added.<sup>19</sup> Finally, 800  $\mu\text{L}$  of aqueous 0.03M  $\text{NaBH}_4$  was added immediately until the formation of a red color. The products of each synthesis step were stored at 27–29 °C and characterized using UV–Vis spectroscopy, Transmission Electron Microscopy (TEM), <sup>1</sup>H-NMR<sup>7</sup> and Raman spectroscopy. The “as-prepared” DOX IN PEG-AuNPs solution was centrifuged at 10,000 rpm for 10 min for three times; then, the supernatant was discarded. This procedure was repeated twice to remove excess non-conjugated dicarboxylic PEG.

### Synthesis of GEM@DOX in PEG-AuNPs

GEM was grafted onto DOX IN PEG-AuNPs through electrostatic bonds between GEM’s amine function of GEM and the carboxylic group ( $\text{COO}^-$ ) of PEG diacide. Briefly, 1mL of GEM (0.01M) was added to 20mL of DOX in PEG-AuNPs (0.1M) and magnetically stirring for 18h at room temperature. The formation of GEM@DOX in PEG-AuNPs was observed as a progressive color change of the solution from bright orange-violet to blue over 18h. The products of each synthetic step were stored at 27–29 °C and characterized using UV–Vis spectroscopy and Transmission Electron Microscopy (TEM). The “as-prepared” GEM@DOX IN PEG-AuNPs solution was purified by dialysis.

### Preparation of Galectin Protein Solutions (Gal-I)

Galectin powder was diluted in water at different concentrations within the range of 1  $\mu\text{M}$  to 1 pM, and the molar concentration of Galectin-1 was estimated to be 14,716 Da.

### Bioconjugation of GEM@DOX in PEG-AuNPs with Gal-I

The interaction of Gal-1 protein with the GEM@DOX IN PEG-AuNPs surface was obtained by exploiting the procedures previously discussed.<sup>13</sup>

Briefly, 5 mL of GEM@DOX IN PEG-AuNPs (42nM) was added to separate tubes containing 50  $\mu$ L Gal-1 (10  $\mu$ M to 1 pM; PBS pH 7; NaCl 0.15 M). After 18 h of incubation, the GEM@DOX IN PEG-AuNPs/Gal-1 suspension was centrifuged twice at 5000 rpm for 10 min to eliminate excess Gal-1, and the pellets were redispersed in 1 mL of Milli-Q water as described previously.<sup>13</sup>

## Physicochemical Characterization

All measurements were performed in triplicates to validate the reproducibility of the synthetic and analytical procedures. All the measurements were performed as previously described.<sup>7</sup>

## UV/Vis Measurements

Absorption spectra were recorded using a Kontron UV 941 spectrophotometer in plastic cuvettes with an optical path of 10 mm. The wavelength range was 200–900 nm.

## Transmission Electron Microscopy (TEM)

All microscopy analyses were realized as previously described.<sup>7</sup>

## Raman Spectroscopy

Raman spectroscopy was performed using an Xplora spectrometer (Horiba Scientific, France). The Raman spectra were recorded at an excitation wavelength of 785 nm (diode laser) at room temperature. For the measurements in the solution, a macro-objective with a focal length of 40 mm (NA = 0.18) was used in the backscattering configuration. The spectral resolution achieved was approximately 2  $\text{cm}^{-1}$ .

## Dynamic Light Scattering (DLS)

Size measurements were performed at room temperature using a Zetasizer Nano ZS (Malvern Instruments, Malvern, UK) equipped with a He-Ne laser (633 nm, fixed scattering angle of 173°).

Zeta potential measurements: All measurements were carried out as previously described.<sup>7,13</sup>

DOX /GEM loading efficiency: The amount of drug incorporated into PEG-AuNPs was measured using UV–Vis absorption spectroscopy, as described previously.<sup>9</sup>

DOX/GEM release: DOX and GEM release was evaluated at physiological temperature (37 °C). Experimental conditions are described in a previous work of some of the authors.<sup>9,19</sup>

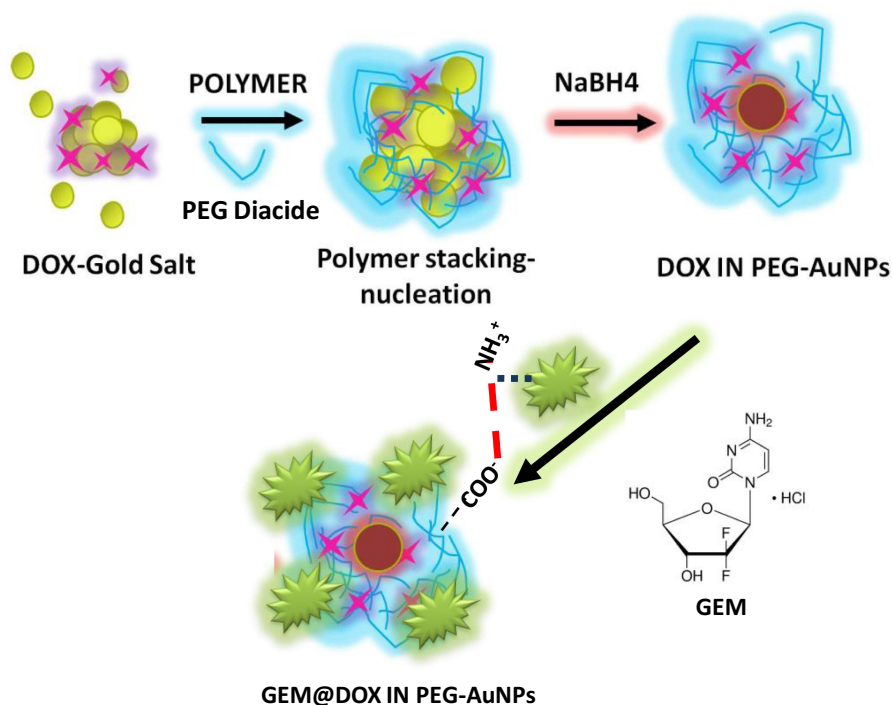
## Results and Discussion

### Formation Mechanism of GEM@DOX in PEG-AuNPs

Previously, Moustauoui et al conceived a novel doxorubicin nanotherapeutic agent obtained by methodology IN.<sup>7</sup> This methodology has been applied to several drugs and biomolecules to understand the mechanism of hybrid nanoparticles and the competitive effect between several capping agents and drugs on the growth process of gold nanoparticles.<sup>8,9,20,21</sup> These authors have applied this methodology on gemcitabine (GEM) in which the original nanoflower shapes are produced after the growth process.

The aim of this study was to demonstrate the formation of stable complexes of PEGylated Au(III)-DOX AuNPs before and after grafting of gemcitabine (GEM) to form a hybrid chemotherapeutic nanovector. The synthesis process involved three steps (Scheme 1).

1. Synthesis of DOX from PEG-AuNPs by complexation protocol (Method IN) and reduction with  $\text{NaBH}_4$ .
2. Electrostatic grafting of gemcitabine onto DOX in PEG-AuNPs via amino groups ( $\text{NH}_3^+$ ) of the GEM and carboxylic group ( $\text{COO}^-$ ) of the PEG diacide polymer at higher concentrations.
3. Stabilization of hybrid nanovector (GEM@DOX IN PEG-AuNPs).



**Scheme 1** Synthesis and electrostatic grafting of gemcitabine (GEM) to DOX IN PEGAuNPs obtained by methodology IN.<sup>7</sup>

In the first step, DOX molecules were added to the  $\text{HAuCl}_4$  aqueous solution, and the biocompatible polymer was added to form DOX IN PEG-AuNPs, as previously described.<sup>7</sup> In the second step, GEM was adsorbed electrostatically onto DOX IN PEG-AuNPs via amino groups under experimental conditions and chemical stabilization (third step). All products of our synthetic procedure were assessed using UV-Vis absorption<sup>22</sup> spectroscopy, TEM<sup>18</sup> and Raman Spectroscopy.

## Comparative Physico-Chemical Characterization of GEM@DOX in-PEG-AuNPs

TEM images of GEM@DOX IN PEG-AuNPs showed good dispersion of the nanoparticles, with an average size of  $33 \pm 7.2\text{nm}$  (Figure 1A). Spadavecchia et al reported the synthesis of GEM ION PEG-AuNPs, such as snowflake nanoparticles, obtained after the nanoparticle process. Based on previously reported findings, we supposed that when GEM was added to DOX in PEG-AuNPs solution, the GEM molecules were in J conformation<sup>23</sup> and the concentration was optimal to arrange the better conformation in order to interact with the carboxylic group of PEG diacide to obtain spherical nanoparticles with high stability.

The absorption spectra of GEM@DOX IN PEG-AuNPs were evaluated with a small peak at 300 nm, assigned to PEG diacide absorption and a surface plasmon band at 555 nm (Figure 1A). The stability of AuNPs was confirmed by DLS measurements (Data Showed In [Supporting Information Section](#)). Zeta potential measurements showed that GEM@DOX IN PEG-AuNPs were stable at physiological pH (z-potential =  $-28 \pm 1\text{ mV}$ ; Data Showed In [Supporting Information](#)).

The steric arrangement of GEM on DOX pegylated AuNPs was confirmed by Raman spectroscopic analysis (Figure 1C).

The Raman spectra of free DOX, GEM, and GEM@DOX IN PEG-AuNPs in water exhibited several bands in the region  $500\text{--}3000\text{ cm}^{-1}$  (Figure 1C). The Raman spectra of free DOX (Figure 1C, red line) and DOX IN PEG-AuNPs (Figure 1C, blue line) in water show many peaks as fingerprints of the hybrid nanosystem as previously described.<sup>7,10</sup> Focusing our attention on the spectral range  $200\text{--}500\text{ cm}^{-1}$  and  $2000\text{--}3100\text{ cm}^{-1}$ , several spectral changes were detected, which confirmed the chemical and steric modification of each drug (GEM; DOX) after complexation with gold ions and PEG-diacide molecules. The presence of PEG-diacide at the surface of the AuNPs was confirmed by the Raman bands at

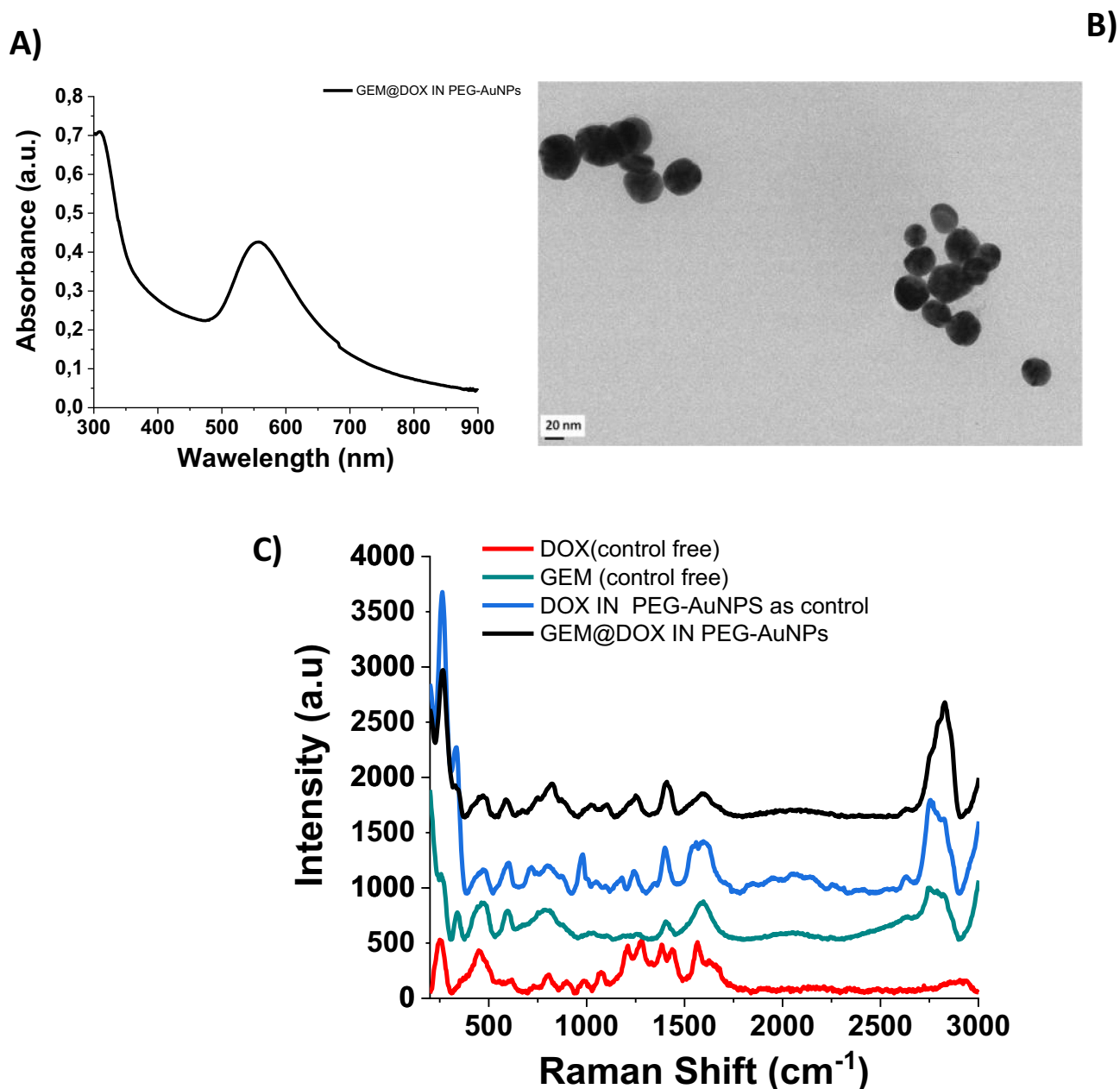


**Figure 1** (A) UV-Vis absorption of GEM@DOX IN PEG-AuNPs (B) TEM images of GEM@DOX IN PEG-AuNPs and (C) Raman spectra of the GEM@DOX IN PEG-AuNPs products compared to free GEM (green line), free DOX (red line) and DOX IN PEG-AuNPs (blue line) as controls. (A and B) Scale bars: 20nm.

1137 cm<sup>-1</sup>, 1270 cm<sup>-1</sup>, and 1455 cm<sup>-1</sup> due to the vibrations of C-O-H, C-O-C, and C-O chemical groups, respectively. The Raman spectra of free GEM (Figure 1C; green line) and GEM@DOX IN-PEG-AuNPs (Figure 1C, black line) in water also exhibited several bands in the region of 500–2000 cm<sup>-1</sup>. In particular, the peak at 821 cm<sup>-1</sup> characteristic of the aromatic proton and C-F groups, the vibrations at 1250 cm<sup>-1</sup> and 1400 cm<sup>-1</sup> were due to  $\nu$  C-O-C stretching, and the vibration at 1655 cm<sup>-1</sup> was due to the protonated amino group. We observed a decrease in the peak at 335 cm<sup>-1</sup> due to the C-N vibrations of the piperazynil group. In contrast, with the Raman spectra of the GEM ION PEG AuNPs conceived previously, we noted the presence of bands located between 469 and 514 cm<sup>-1</sup> due to the C-C-O vibration. The prominent peak at 339 cm<sup>-1</sup> due to the vibrations  $\delta$ (OH...O) and  $\nu$ (OH...O) of PEG disappeared. Based on these and previous spectrochemical results, we identified that GEM grafted electrostatically onto DOX IN PEG-AuNPs assumes a better chemical conformation, in which the amino group (NH<sub>3</sub><sup>+</sup>) reacts with the carboxylic (COO<sup>-</sup>) group of PEG

diacide, whereas the cyclopentanol group at position C-5' reacts with  $\text{NH}_3^+$  of DOX. We also observed more peaks in the region between  $1000\text{ cm}^{-1}$  and  $1200\text{ cm}^{-1}$  and an exaltation of the band at  $2888\text{ cm}^{-1}$  due to CH stretching and the chemical and steric arrangement of GEM on DOX IN PEG-AuNPs.

## Galectin Active Interaction: Spectroscopic Evaluation

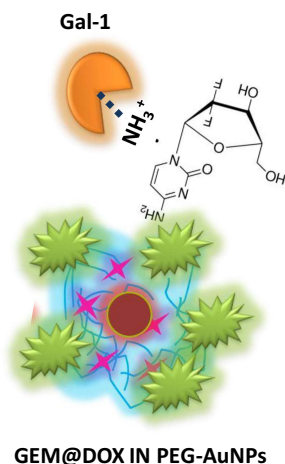
Galectins are glycan-binding proteins with a high affinity for  $\beta$ -galactosides owing to the presence of characteristic carbohydrate recognition domains (CRDs)<sup>24</sup> responsible for specific biological responses.<sup>25</sup>

Previously, we used chitlac pegylated gold nanoparticles (CTL-PEG-AuNPs) as building blocks to observe biomolecular interaction with Galectin-1 (Gal-1) and the relationship between chemical structure and biological activity.<sup>13</sup> Herein, we tested the capacity of interaction between Gal-1 and GEM@DOX in PEG-AuNPs to understand the relationship between the drug nanovector and biomarker. Gal-1 proteins were incubated with different concentrations of AuNP solutions (Scheme 2). Gal-1 interacts with GEM@DOX in PEG-AuNPs, as shown by SPR and Raman measurements (Figure 1). When Gal-1 was added to GEM@DOX IN PEG-AuNPs, we observed a dynamic variation in the plasmon position with Gal-1 concentration (from  $10^{-6}\text{ M}$  to  $10^{-12}\text{ M}$ ) (Figure 2). As discussed previously, the interaction of Gal-1 with the gold surface of GEM@DOX in PEG-AuNPs leads to the agglomeration of the colloidal solution. The weak red shift and strong decrease in the plasmon band can be explained by lower nanoparticle aggregation and dissociation of agglomerates.<sup>13</sup> From  $10^{-6}\text{ M}$  ( $1\text{ }\mu\text{M}$ ) to  $10^{-12}\text{ M}$  ( $1\text{ pM}$ ), Gal-1 interacted with the GEM@DOX IN PEG-AuNPs, inducing a decrease in the plasmon band with a consequent modification of the dielectric constant around the AuNPs after interaction with Gal-1 proteins. At concentrations higher than  $1\text{ nM}$ , more Gal-1 molecules interacted with GEM@DOX IN PEG-AuNPs, forming a Gal-1 monolayer on the AuNP surface. At a concentration of  $1\text{ nM}$ , the amount of Gal-1 was large enough to prevent any interactions between the proteins in the GEM@DOX IN PEG-AuNPs, thus inducing dissociation of the nanoparticle agglomerates. With the saturation of the surface of the AuNPs, we can suppose that it could induce a better orientation of Gal-1 or a change in its conformation owing to chemical hindrance and protein conformational changes with the chemical group of GEM.

## Galectin Active Interaction : Raman Spectroscopy Assessment

A fruitful interaction of Gal-1 with the GEM@DOX IN PEG-AuNPs surface was also achieved by Raman spectroscopy (Figure 3).

Raman spectroscopy is a vibrational spectroscopy technique that can be applied to study the molecular structure of several proteins before and after interaction with AuNPs under specific conditions.<sup>26</sup> The influence of hydrophobic



**Scheme 2** Representation of interaction mechanism of Galectin-1 onto GEM@DOX IN PEG-AuNPs and subsequent conformational change of galectin molecules under specific concentrations of protein.

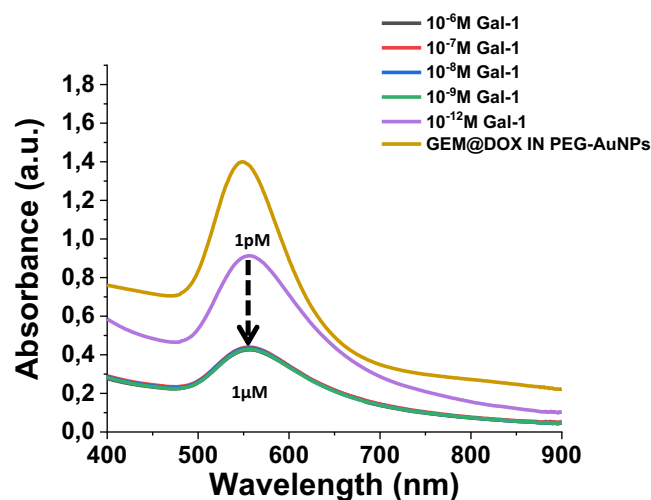


**Figure 2** UV-Vis absorption spectra in the range 200–900 nm of GEM@DOX IN PEG-AuNPs before (yellow line) and after interaction of Galectin-I (from 1  $\mu$ M to 1 pM) under straight condition (NaCl 0.9%).

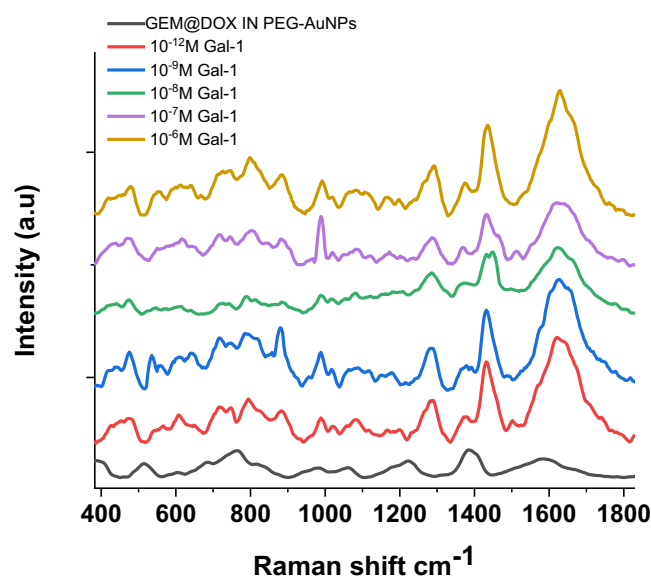


**Figure 3** Raman spectra of GEM@DOX IN PEG-AuNPs before (black line) and after interaction of Gal-I (Galectin-I concentration range 1  $\mu$ M - 1 pM). Experimental conditions:  $\lambda_{exc}$  = 785 nm; laser power 20 mW; accumulation time 180 s.

interactions between proteins is also discussed.<sup>27</sup> Indeed, the intensity and frequency of the vibrational groups of the amino acid side chains and polypeptide backbone are susceptible to chemical modifications of the microenvironment.<sup>28</sup>

After the Gal-1 binding, amide II (1587–1620  $\text{cm}^{-1}$ ) and amide III (1200–1300  $\text{cm}^{-1}$ ), as well as modifications in the *protein* local environment, confirmed the protein interaction (Figure 3). When the protein concentration was decreased from 500 nM to 1 pM, the fingerprint of the amide band was masked by the water peak at 1600  $\text{cm}^{-1}$  due to the ionic environment.

As mentioned previously,<sup>13</sup> the chemical and steric conformations of Gal-1 depend on the molecular concentration that influences the high packing density and self-assembly of Gal-1 on the chitlac gold nanoparticles (CTL-PEG-AuNPs). Herein, we realized a novel system in which the chemical combination of DOX and GEM, as GEM@DOX IN PEG-AuNPs, influences and simulates the presence of CTL polymer-like bioreceptors of Gal-1 with optimal results. In fact, the self-assembly of Gal-1 onto GEM@DOX IN PEG-AuNPs from 1  $\mu$ M to 1 nM shows characteristic amide bands, and

we observed a change in the chemical fingerprint of the amide bands as a function of concentration. This spectroscopic behavior was probably due to the steric and chemical arrangement between the chemical groups of DOX, GEM (C-O, C-F, and-OH), and Gal-1 at low concentrations.

A notable finding was the increase in the number of peaks in the Raman spectra following the addition of Gal-1. The large fluctuation in the band around  $1600\text{ cm}^{-1}$  displayed a tendency as the Gal-1 concentration increased, which is particularly interesting. An analogous pattern was observed for the band located at  $1400\text{ cm}^{-1}$ . Upon the addition of Gal-1, the spectra also showed a clear shift in the direction of the higher frequencies. These spectroscopic variations highlight Gal-1's tremendous impact on molecular organization in the Raman spectra. Additionally, the presence of Gal-1 might affect the Raman frequencies by changing the local electrical environment near GEM@DOX in PEG-AuNPs molecules. This shifting phenomenon may be influenced by changes in the electron charge distribution or electrostatic interactions. In conclusion, the finding of a shift towards higher frequencies in the Raman spectra after the addition of Gal-1 indicates changes in the electrical environment and molecular interactions. This provided insightful information about the changes in Gal-1 caused by the GEM@DOX IN PEG-AuNPs system.<sup>29</sup>

The spectral region between  $2700$  and  $3000\text{ cm}^{-1}$  corresponds to the stretching vibrations of the hydrogen and C-H bonds. Interestingly, between  $2700$  and  $3000\text{ cm}^{-1}$ , a broad band was observed in the Raman spectrum of GEM@DOX in PEG-AuNPs (Figure 4 black line). After the interaction of Gal-1 at  $10^{-6}\text{ M}$  (Figure 4 yellow line), a strong variation in the Raman spectral bands appeared. In particular, we noted the appearance of the peak at  $2717\text{ cm}^{-1}$  due to the C-H stretching vibration of amino acids related to hydrophobic groups and a strong improvement in the bands at  $2836\text{ cm}^{-1}$ ,  $2886\text{ cm}^{-1}$  and  $2916\text{ cm}^{-1}$  characteristic of  $\text{CH}_2\text{-CH}_3$  symmetrical stretching, and  $\text{CH}_2\text{-CH}_3$  asymmetrical stretching. At  $10^{-7}\text{ M}$  we observed a decrease in these bands, which confirmed the steric arrangement of Ga-1 on the nanoparticles. At  $10^{-12}\text{ M}$  (1pM), we can see an improvement and vibrational shift of the bands at  $2710\text{ cm}^{-1}$ ,  $2836\text{ cm}^{-1}$ ,  $2875\text{ cm}^{-1}$  and  $2916\text{ cm}^{-1}$  due to aromatic and aliphatic amino acids.<sup>30</sup> Nevertheless, it has been previously discussed that a number of charged amino acids, such as lysine, glutamic aspartic acids, proline, threonine, and histidine, also involves signals in the C-H stretching region due to the presence of CH groups and other  $\text{CH}_3$  or  $\text{CH}_2$  group symmetrical stretching. Furthermore, aromatic and aliphatic amino acids had prominent C-H stretching bands, particularly in the main band near  $2935\text{--}2955\text{ cm}^{-1}$ .<sup>30</sup>

The low-frequency Raman bands ( $100\text{--}400\text{ cm}^{-1}$ ) (Figure 5) reflect the collective vibrations of some proteins in aqueous solutions and relatively liquid amides. After Gal-1 interaction with GEM@DOX IN PEG-AuNPs, we observed a strong improvement in the bands around  $100\text{ cm}^{-1}$  due to hydrogen bonds,<sup>31</sup> reflecting the key influence of protein

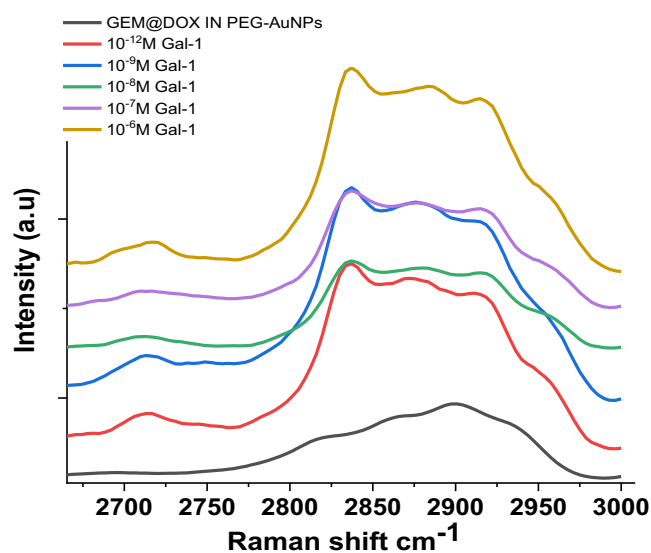


**Figure 4** Magnification of Raman spectra in the  $2700\text{--}3000\text{ cm}^{-1}$  spectral range of GEM@DOX IN PEG-AuNPs before (black line) and after interaction of Gal-1 (Galactin-1 concentration range  $1\text{ }\mu\text{M}$  -  $1\text{ pM}$ ). Experimental conditions:  $\lambda_{\text{exc}} = 785\text{ nm}$ ; laser power  $20\text{ mW}$ ; accumulation time  $180\text{ s}$ .



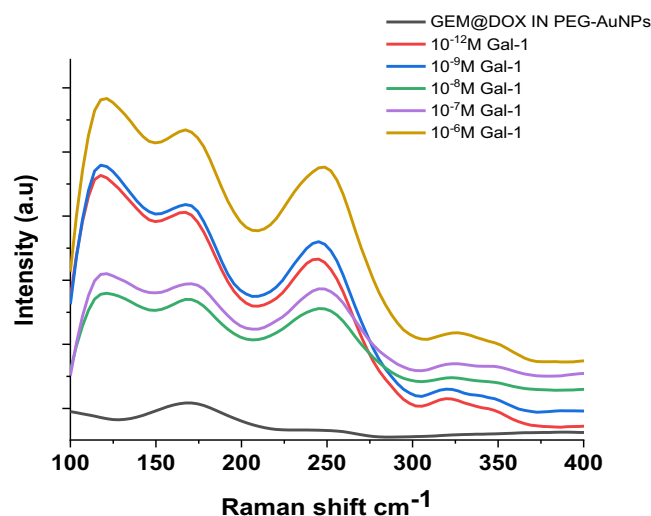


**Figure 5** Magnification of Raman spectra in the 100–400  $\text{cm}^{-1}$  spectral range of GEM@DOX IN PEG-AuNPs before (black line) and after interaction of Gal-1 (Galactin-1 concentration range 1  $\mu\text{M}$  - 1 pM). Experimental conditions:  $\lambda_{\text{exc}} = 785 \text{ nm}$ ; laser power 20 mW; accumulation time 180 s.

concentration on our gold nanoparticle system and their interaction. The bands with maxima at approximately 290  $\text{cm}^{-1}$  and 250  $\text{cm}^{-1}$  might be sensitive to the water structure in aqueous protein solutions.

## Conclusions

In this study, we conceived and realized, for the first time, an original nano-drug delivery system for the bio-interaction between Galectin-1 and PEGylated gold nanoparticles decorated with doxorubicin (DOX) and gemcitabine (GEM) (GEM@DOX IN PEG-AuNPs). The chemical design of nano-drug delivery system was assessed and monitored by UV-visible and Raman spectra, confirming the “good” binding affinity between Gal-1 and GEM@DOX IN PEG-AuNPs. This preliminary study opens further way in order to built “smart nanomedical devices” that could have a dual application as therapeutic and diagnostic in the field of nanomedicine and preclinical studies associated. Further studies are still envisaged, in order to assure the in vitro and/or in vivo assessment toxicity, pharmacokinetics and dynamics on relevant pancreatic-cancer model (PDAC).

## Acknowledgments

We thank “Ligue contre le Cancer” for financing MemonakHAN’s thesis and making it possible to develop this work.

## Author Contributions

All authors made a significant contribution to the work reported, whether that is in the conception, study design, execution, acquisition of data, analysis and interpretation, or in all these areas; took part in drafting, revising or critically reviewing the article; gave final approval of the version to be published; have agreed on the journal to which the article has been submitted; and agree to be accountable for all aspects of the work.

## Disclosure

The authors report no conflicts of interest in this work.

## References

1. Yang Y, Zheng X, Chen L, et al. Multifunctional gold nanoparticles in cancer diagnosis and treatment. *Int J Nanomed.* 2022;17:2041–2067. doi:10.2147/IJN.S355142
2. Yang Z, Wang D, Zhang C, et al. The applications of gold nanoparticles in the diagnosis and treatment of gastrointestinal cancer. *Front Oncol.* 2022;11:819329. doi:10.3389/fonc.2021.819329

3. Singh P, Pandit S, Mokkapat V, Garg A, Ravikumar V, Mijakovic I. Gold nanoparticles in diagnostics and therapeutics for human cancer. *Int J Mol Sci.* 2018;19:7. doi:10.3390/ijms19071979
4. Medici S, Peana M, Coradduzza D, Zoroddu MA. Gold nanoparticles and cancer: detection, diagnosis and therapy. *Semi Cancer Biol.* 2021;76:27–37. doi:10.1016/j.semcancer.2021.06.017
5. García Calavia P, Bruce G, Pérez-García L, Russell DA. Photosensitizer-gold nanoparticle conjugates for photodynamic therapy of cancer. *Photochem Photobiol Sci.* 2018;17(11):1534–1552. doi:10.1039/c8pp00271a
6. Cheng Y, Samia AC, Meyers JD, Panagopoulos I, Fei B, Burda C. highly efficient drug delivery with gold nanoparticle vectors for in vivo photodynamic therapy of cancer. *J Am Chem Soc.* 2008;130(32):10643–10647. doi:10.1021/ja801631c
7. Kashyap BK, Singh VV, Solanki MK, Kumar A, Ruokolainen J, Kesari KK. Smart Nanomaterials in Cancer Theranostics: challenges and Opportunities. *ACS Omega.* 2023;8(16):14290–14320. doi:10.1021/acsomega.2c07840
8. Seidu TA, Kutoka PT, Asante DO, Farooq MA, Alolga RN, Bo W. Functionalization of nanoparticulate drug delivery systems and its influence in cancer therapy. *Pharmaceutics.* 2022;14(5):5. doi:10.3390/pharmaceutics14051113
9. Moustaoi H, Movia D, Dupont N, et al. Tunable Design of Gold(III)–Doxorubicin Complex–PEGylated Nanocarrier. The golden doxorubicin for oncological applications. *ACS Appl Mater Interfaces.* 2016;8(31):19946–19957. doi:10.1021/acsami.6b07250
10. Sahli F, Courcelle M, Palama T, Djaker N, Savarin P, Spadavecchia J. Temozolomide, gemcitabine, and decitabine hybrid nanoconjugates: from design to proof-of-concept (PoC) of synergies toward the understanding of drug impact on human glioblastoma cells. *J Med Chem.* 2020;63(13):7410–7421. doi:10.1021/acs.jmedchem.0c00694
11. Liu H, Jiang P, Li Z, Li X, Djaker N, Spadavecchia J. HIV-1 tat peptide-gemcitabine gold (III)-PEGylated Complex—Nanoflowers: a Spleek Thermosensitive hybrid nanocarrier as prospective anticancer. *Part Part Syst Charact.* 2018;35(8):1800082. doi:10.1002/ppsc.201800082
12. Arib C, Spadavecchia J, de la Chapelle ML. Enzyme mediated synthesis of hybrid polyedric gold nanoparticles. *Sci Rep.* 2021;11(1):3208. doi:10.1038/s41598-021-81751-1
13. Liu Q, Liu H, Sacco P, et al. Correction: CTL–doxorubicin (DOX)–gold complex nanoparticles (DOX–AuGCs): from synthesis to enhancement of therapeutic effect on liver cancer model. *Nanoscale Adv.* 2022;4(21):4701–4702. doi:10.1039/D2NA90075K
14. Khan M, Boumati S, Arib C, et al. Doxorubicin (DOX) gadolinium-gold-complex: a new way to tune hybrid nanorods as theranostic agent. *Int J Nanomed.* 2021;16:2219–2236. doi:10.2147/IJN.S295809
15. Liu Q, Sacco P, Marsich E, et al. Lactose-modified chitosan gold(III)-PEGylated complex-bioconjugates: from synthesis to interaction with targeted galectin-1 protein. *Bioconjug Chem.* 2018;29(10):3352–3361. doi:10.1021/acs.bioconjchem.8b00520
16. Liu Q, Aouidat F, Sacco P, Marsich E, Djaker N, Spadavecchia J. Galectin-1 protein modified gold (III)-PEGylated complex-nanoparticles: proof of concept of alternative probe in colorimetric glucose detection. *Colloids Surf B Biointerfaces.* 2020;185(110588):15. doi:10.1016/j.colsurfb.2019.110588
17. Mariño KV, Cagnoni AJ, Croci DO, Rabinovich GA. Targeting galectin-driven regulatory circuits in cancer and fibrosis. *Nat Rev Drug Discov.* 2023;22(4):295–316. doi:10.1038/s41573-023-00636-2
18. Camby I, Le Mercier M, Lefranc F, Kiss R. Galectin-1: a small protein with major functions. *Glycobiology.* 2006;16(11):13. doi:10.1093/glycob/cw1025
19. Thijssen VLJL, Postel R, Brandwijk RJMGE, et al. Galectin-1 is essential in tumor angiogenesis and is a target for antiangiogenesis therapy. *Proc Natl Acad Sci.* 2006;103(43):15975–15980. doi:10.1073/pnas.0603883103
20. Qin H, Qin B, Yuan C, Chen Q, Xing D. Pancreatic Cancer detection via Galectin-1-targeted Thermoacoustic Imaging: validation in an *in vivo* heterozygosity model. *Theranostics.* 2020;10(20):9172–9185. doi:10.7150/thno.45994
21. Capasso D, Pirone L, Di Gaetano S, et al. Galectins detection for the diagnosis of chronic diseases: an emerging biosensor approach. *TrAC Trend Analytical Chem.* 2023;159:116952. doi:10.1016/j.trac.2023.116952
22. Yoshioka K, Sato Y, Murakami T, Tanaka M, Niwa O. One-step detection of galectins on hybrid monolayer surface with protruding lactoside. *Anal Chem.* 2010;82(4):1175–1178. doi:10.1021/ac9022346
23. van Beijnum JR, Thijssen VL, Lämpchen T, et al. A key role for galectin-1 in sprouting angiogenesis revealed by novel rationally designed antibodies. *Internat J Can.* 2016;139(4):824–835. doi:10.1002/ijc.30131
24. Spadavecchia J, Apchain E, Albéric M, Fontan E, Reiche I. One-step synthesis of collagen hybrid gold nanoparticles and formation on Egyptian-like gold-plated archaeological ivory. *Angew Chem Int Ed.* 2014;53(32):8363–8366. doi:10.1002/anie.201403567
25. Maurizio C, Flavio R, Maria Enrica DP, Elena T, Giuseppina DL. Conformational features of 4-(N)-squalenoyl-gemcitabine in solution: a combined NMR and molecular dynamics investigation. *New J Chem.* 2015;39(5):3484–3496. doi:10.1039/C4NJ02091J
26. Johannes L, Wunder C, Shafaq-Zadah M. Glycolipids and lectins in endocytic uptake processes. *J Mol Biol.* 2016. doi:10.1016/j.jmb.2016.10.027
27. Cousin JM, Cloninger MJ. The role of galectin-1 in cancer progression, and synthetic multivalent systems for the study of galectin-1. *Int J Mol Sci.* 2016;17(9):1566. doi:10.3390/ijms17091566
28. Marcon P, Marsich E, Vetere A, et al. The role of Galectin-1 in the interaction between chondrocytes and a lactose-modified chitosan. *Biomaterials.* 2005;26(24):4975–4984. doi:10.1016/j.biomaterials.2005.01.044
29. Rwere F, Mak PJ, Kincaid JR. Resonance Raman interrogation of the consequences of heme rotational disorder in myoglobin and its ligated derivatives. *Biochemistry.* 2008;47(48):12869–12877. doi:10.1021/bi801779d
30. Liu J, Peng Q. Protein-gold nanoparticle interactions and their possible impact on biomedical applications. *Acta Biomater.* 2017;55:13–27. doi:10.1016/j.actbio.2017.03.055
31. Pace CN, Fu H, Fryar KL, et al. Contribution of hydrophobic interactions to protein stability. *J Mol Biol.* 2011;408(3):514–528. doi:10.1016/j.jmb.2011.02.053

Nanotechnology, Science and Applications

Dovepress

### Publish your work in this journal

Nanotechnology, Science and Applications is an international, peer-reviewed, open access journal that focuses on the science of nanotechnology in a wide range of industrial and academic applications. It is characterized by the rapid reporting across all sectors, including engineering, optics, bio-medicine, cosmetics, textiles, resource sustainability and science. Applied research into nano-materials, particles, nano-structures and fabrication, diagnostics and analytics, drug delivery and toxicology constitute the primary direction of the journal. The manuscript management system is completely online and includes a very quick and fair peer-review system, which is all easy to use. Visit <http://www.dovepress.com/testimonials.php> to read real quotes from published authors.

Submit your manuscript here: <https://www.dovepress.com/nanotechnology-science-and-applications-journal>